Complexity of Mesoscale Eddy Diffusivity in the Ocean

Igor Kamenkovich[1], Pavel Berloff[2], Michael Haigh[2], Luolin Sun[2], and Yueyang Lu[1]

[1]Rosenstiel School of Marine and Atmospheric Sciences, University of Miami, Miami, FL 33149, USA. [2] Department of Mathematics, Imperial College London, London, United Kingdom

Corresponding author: Igor Kamenkovich (ikamenkovich@miami.edu)

Key Points:

- Transports of oceanic tracers by mesoscale currents in climate models need to be represented using eddy diffusivity and tracer gradients
- Numerical simulations demonstrate that this diffusivity tensor is space-, time-, direction- and tracer-dependent
- These properties can lead to upgradient eddy fluxes and the importance of all tensor components

Abstract

Stirring of water by mesoscale currents ("eddies") leads to large-scale transport of many important oceanic properties ("tracers"). These eddy-induced transports can be related to the large-scale tracer gradients, using the concept of turbulent diffusion. The concept is widely used to describe these transports in the real ocean and to represent them in climate models. This study focuses on the inherent complexity of the corresponding eddy diffusivity tensor, defined here in all its spatio-temporal complexity. Results demonstrate that this comprehensive diffusivity tensor is space-, time-, direction- and tracer-dependent. Using numerical simulations with both idealized and comprehensive models of the Atlantic circulation, we show that these properties lead to upgradient eddy fluxes and the potential importance of all tensor components. Implications of all this complexity for the development of eddy parameterization schemes in climate models and diffusivity estimates are discussed.

Plain Language Summary

Mesoscale eddies, loosely defined as ocean currents on the spatial scales of tens to hundreds of kilometers, are ubiquitous in the World Ocean. Relentless stirring of water by these eddies leads to large-scale transport and redistribution of many dynamically and climatically important oceanic properties. The efficiency of this process has been conventionally quantified by turbulent ("eddy") diffusion. Our study focuses on the inherent complexity of the corresponding eddy diffusivity tensor, defined here in all its spatio-temporal complexity, without any space and/or time averaging. Results from this study demonstrate that this diffusivity tensor is space-dependent (inhomogeneous), time-dependent (non-stationary) and direction-dependent (anisotropic). Using numerical simulations with both idealized (quasigeostrophic) and comprehensive (primitive-equation) models of the North Atlantic circulation, we show that these properties lead to upgradient eddy fluxes, that is, to negative eigenvalues of the diffusivity tensor. We also show that all components of the comprehensive tensor are potentially important for tracer distributions, and, therefore, cannot be generally neglected. Our results further demonstrate that the comprehensive diffusivity tensor is tracer-dependent and, therefore, non-unique. Implications of all this complexity for the development of eddy parameterization schemes and diffusivity estimates are discussed.

1 Introduction

Mesoscale eddies, loosely defined as ocean currents on the spatial scales of tens to hundreds of kilometers, are ubiquitous in the World Ocean (Chelton *et al.*, 2007). Relentless stirring of water by these eddies leads to large-scale transport and redistribution of many dynamically and climatically important oceanic properties ("tracers"), including heat, salinity and anthropogenic carbon. As a result, mesoscale eddies play a key role in determining the current and future states of the World Ocean and Earth Climate, as manifested by strong sensitivity of ocean and climate simulations to the magnitude and distribution of eddy transports (Gnanadesikan *et al.*, 2013; McWilliams, 2008; Wiebe & Weaver, 1999). At the same time, vast majority of ocean component in modern climate models either completely miss the eddies or only partially resolve them (Delworth *et al.*, 2012; Williams *et al.*, 2015). The eddy-induced transports in these models need to be expressed ("parameterized") in terms of known large-scale properties. This task requires a thorough study of eddy transport properties and their significance for tracer distributions. This study reports several new properties of the eddy transport, using the framework of turbulent eddy diffusivity, which is defined next.

By analogy between this turbulent transport and molecular diffusion, the corresponding flux $\boldsymbol{F}(x,y,z,t)$ of a tracer c can be written as a linear function of the large-scale tracer gradient(Prandtl, 1925; Taylor, 1921; Vallis, 2017):

$$\boldsymbol{F} = -\boldsymbol{K}\nabla\langle c\rangle \tag{1}$$

where $\mathbf{K}$ is the eddy diffusivity tensor and the angle brackets denote the large-scale component of a field. This eddy diffusivity, with some common simplifications, has been traditionally used in numerical models to represent ("parameterize") turbulent fluxes due to the important unresolved part of the flow. The divergence of the eddy flux enters the tracer equation, along with advection by the large-scale flow:

$$\frac{\partial c}{\partial t} + \nabla\cdot(\langle \boldsymbol{u}\rangle\langle c\rangle) = -\nabla\cdot\boldsymbol{F}, \qquad \text{where } \boldsymbol{F} = \langle \boldsymbol{u}\rangle c' + \boldsymbol{u}'\langle c\rangle + \boldsymbol{u}'c' \tag{2}$$

The eddy flux divergence $\nabla\cdot\boldsymbol{F}$ can play a key role in determining tracer evolution and steady state. For simplicity, we assume that the tracer is conservative, thus ignoring sources and sinks, and focus only on dynamically passive tracers, thus assuming that the ocean currents are not affected by c.

Because of the joint effect of planetary rotation and ocean stratification, the stirring of water by mesoscale eddies is primarily along surfaces of constant density (isopycnals) in the interior ocean. Therefore, the main focus here is on the *lateral* material transport. The general eddy diffusivity tensor **K** in a 2D flow can be written as a 2×2 matrix:

$$\boldsymbol{K}(x, y, t) = \begin{pmatrix} K_{xx} & K_{xy} \\ K_{yx} & K_{yy} \end{pmatrix}, \tag{3}$$

where the conventional Cartesian coordinates are used for convenience. Note that a pair of tracers is needed for a solution of Equation 1, and for that pair the solution is exact and unique.

The seeming simplicity of the flux-gradient relation (Equation 1) hides incredible complexity of the diffusivity tensor **K**. Only in purely homogeneous, stationary and isotropic turbulence are the off-diagonal tensor zero (K_{xy}=K_{yx}=0) and the diagonal tensor elements equal to each other (K_{xx}=K_{yy}). In realistic oceanic flows, all **K**-tensor elements are generally non-zero, distinct (i.e., the diffusivity is *anisotropic*) and vary in space and time (i.e., the diffusivity is *inhomogeneous and non-stationary*). Observation- and model-based estimates of the simplified eddy diffusivity exhibit strong dependence on depth, geographical location (Abernathey & Marshall, 2013; Canuto *et al.*, 2019; Cole *et al.*, 2015; Griesel *et al.*, 2010; Lumpkin *et al.*, 2002; Marshall *et al.*, 2006) and time (Busecke & Abernathey, 2019; Haigh *et al.*, 2020). These estimates usually involve some spatio-temporal averaging and can be based on either drifter (“particle”) trajectories or tracer distributions. Both particle-based statistics (Griesel *et al.*, 2010; Kamenkovich *et al.*, 2009; Kamenkovich *et al.*, 2015; McClean *et al.*, 2002; O'Dwyer *et al.*, 2000; Rypina *et al.*, 2012; Sallee *et al.*, 2008) and tracer-based estimates (Bachman *et al.*, 2020; Bachman *et al.*, 2017; Eden, 2007; Haigh *et al.*, 2020) also exhibit significant anisotropy. This anisotropy is important in the typical oceanic case of strong eddies embedded in relatively weak large-scale circulation (Kamenkovich *et al.*, 2015).

The diffusion approach (Equation 1) is built on an inherent assumption that the **K-**tensor is unique for any given turbulent flow. However, some model estimates report significant sensitivity of a simplified **K**-tensor to the tracer field (Bachman *et al.*, 2015; 2020; Eden & Greatbatch, 2009; Haigh *et al.*, 2020). This sensitivity complicates interpretation of **K**-tensor, because even the exact solution of (1) for one particular pair of tracers will lead to biases in ***F*** for another set.

The other serious complication is that $\boldsymbol{F}$ contains some large non-divergent ("rotational") component (Haigh *et al.*, 2020; Jayne & Marotzke, 2002; Marshall & Shutts, 1981) that does not affect tracer distribution, but influences $\mathbf{K}$ in the flux-gradient relation (1). The rotational flux can be expected to be tracer-dependent (Bachman *et al.*, 2015) and can lead to negative diffusivities (Marshall & Shutts, 1981). The separation of $\boldsymbol{F}$ into rotational and divergent components via the Helmholtz decomposition is, unfortunately, not unique and depends on the boundary conditions (Jayne & Marotzke, 2002; Maddison *et al.*, 2015; Roberts & Marshall, 2000), which are usually known for the total $\boldsymbol{F}$ but not for its rotational and divergent components, separately.

2 Numerical Simulations

Two types of simulations are used in this study. The first type is the idealized quasigeostrophic (QG) double-gyre flow. This flow contains all essential elements of the mid-latitude North Atlantic or North Pacific: large-scale subpolar and subtropical gyres, separated by a coherent meandering jet, representing eastward extensions of the Gulf Stream and Kuroshio currents, and an ambient eddy field. The model is formulated in a square-box flat-bottom ocean basin, which is a classical idealization that facilitates the analysis and numerical simulations(Haigh *et al.*, 2020). The numerics employs the CABARET scheme (Karabasov *et al.*, 2009) on a uniform Cartesian grid with 1025 by 1025 grid points and the grid spacing $\Delta x = \Delta y = 3.5$ km. The model has 3 vertical layers. The length of the tracer simulations is 180 days.

The second model is a comprehensive, general circulation model (GCM) of the entire Atlantic, used in the “offline” regime, which means that tracers are simulated using previously computed physical fields, thus, making the model computationally very efficient (Kamenkovich *et al.*, 2017). The physical variables used in offline models are calculated in a separate “online” simulation with the HYbrid Coordinate Ocean Model (HYCOM) (Bleck, 2002; Chassignet *et al.*, 2003), which uses isopycnal coordinates in the open ocean and below the mixed layer. HYCOM's coordinate system dynamically transitions to other coordinate types (sigma- and z-coordinates) to provide optimal resolution in the surface mixed layer, in high-latitude unstratified regions, and near coasts. The online simulation has a global domain with $1/12^{\circ}$ spatial resolution; the horizontal grid is rectilinear south of 47°N followed by an Arctic bipolar patch. The vertical grid has 41 hybrid layers. Both model solutions are initialized with 2D tracer configurations which initially are vertically uniform but have different horizontal profiles. The QG model is integrated for 180 days, while the GCM is used for 14 overlapping segments, 110 days each.

3 Tensor calculation and basic properties

The definition of the mean circulation and large-scale tracer field is not unique, and the resulting K-tensor depends significantly on it. The mesoscale is not clearly separated from the large-scale in ocean models and observations(McWilliams, 2008), and an unambiguous definition of the eddies is missing. The large scales are often defined as long-term time mean (Vallis, 2017), although the utility of this definition is far from clear for transient tracers. Thus, a fundamental uncertainty in defining the eddies leads to uncertainty in defining the eddy diffusivity. This study defines mesoscale using spatial filtering, which is relevant to the issue of spatial resolution of essies in numerical models. For example, the QG analysis in this study employs the low-pass spatial filtering <…> intended to remove scales shorter than 112.5 km and does not use time averaging, while the GCM analysis uses a square filter width of approximately 2 degrees longitude and a 5-year mean for the time averaging.

The flux-gradient relation can be solved exactly for any pair of independent tracers. We use 6 linear and 6 nonlinear tracers (15 independent pairs in each set). The linear tracers are linear functions of x and y (constant gradient) with a constant added, which means that solving (1) must produce a unique diffusivity tensor if the rotational component is properly removed (Sun, 2020). This is because that any linear tracer can be expressed as a linear combination of only two independent tracers. In the GCM simulations, we use 4 independent tracers (6 tracer pairs). Each of these tracers decreases exponentially southward from 31°S and northward from the grid point 1800 to 1954 (latitude varies due to curvilinear coordinates used in HYCOM).

The rotational component is removed from each tracer flux, using the Helmholtz decomposition (Lau & Wallace, 1979):

$$\nabla \cdot \boldsymbol{F} = \nabla^2 \Phi, \;\; \nabla \times \boldsymbol{F} = \nabla^2 \Psi,$$
$$\boldsymbol{F} = \boldsymbol{F_{div}} + \boldsymbol{F_{rot}}, \tag{4}$$
$$\boldsymbol{F_{div}} = \nabla \Phi, \;\; \boldsymbol{F_{rot}} = \nabla \times \Psi.$$

In the QG simulations, we adopt the approach of Maddison *et al.* (2015) and set $\Phi = 0$ at the lateral boundaries, which minimizes the magnitude of $\boldsymbol{F_{div}}$. GCM simulations have open boundaries in the north and south, and a different approach is used. We chose to use the optimization technique with Tikhonov regularization (Li *et al.*, 2006), which minimizes the opposing non-rotational and non-divergent in $\boldsymbol{F}_{div}$ and $(\boldsymbol{F}-\boldsymbol{F}_{div})$. Note that $\nabla\cdot\boldsymbol{F}_{div}=\nabla\cdot\boldsymbol{F}$ regardless of the boundary conditions used in the Helmholtz decomposition, although the diffusivity tensor $\mathbf{K}$ is derived from $\boldsymbol{F}_{\boldsymbol{div}}$ and, thus, is highly sensitive to the choice of the boundary conditions.

The diffusivity tensor $\mathbf{K}$ can be decomposed into the symmetric and anti-symmetric components:

$$\boldsymbol{K}=\boldsymbol{K_s}+\boldsymbol{K_a}=\begin{pmatrix}K_{xx} & \mathrm{S}_{12}\\ \mathrm{S}_{12} & K_{yy}\end{pmatrix}+\begin{pmatrix}0 & \mathrm{A}_{12}\\ -\mathrm{A}_{12} & 0\end{pmatrix},\qquad \mathrm{S}_{12}=\frac{1}{2}\left(K_{xy}+K_{yx}\right),\quad \mathrm{A}_{12}=\frac{1}{2}\left(K_{xy}-K_{yx}\right). \tag{5}$$

When the diffusivity is isotropic and inhomogeneous, these two components of the full tensor correspond to the divergent (zero curl and non-zero divergence) and rotational (zero divergence and non-zero curl) components, $-\boldsymbol{K_s}\boldsymbol{\nabla}\langle c\rangle$ and $-\boldsymbol{K_a}\boldsymbol{\nabla}\langle c\rangle$, respectively. It is, however, easy to see that the curl of the symmetric part is non-zero, $\nabla\times\boldsymbol{K_s}\boldsymbol{\nabla}\langle c\rangle\neq 0$, if $\boldsymbol{K_s}$ is anisotropic ($K_{xx}\neq K_{yy}$) or inhomogeneous. Because the rotational component is exactly zero in the full $\boldsymbol{F}_{\boldsymbol{div}}$, the rotational components in symmetric and antisymmetric parts cancel each other. Similarly, the antisymmetric part has non-zero divergence for the inhomogeneous tensor: $\nabla\cdot\boldsymbol{K_a}\boldsymbol{\nabla}\langle c\rangle = J(A,\langle c\rangle)\neq 0$. For example, our QG estimates show that the r.m.s. of the divergence of $\boldsymbol{K}_s\nabla\langle c\rangle$ and $\boldsymbol{K}_a\nabla\langle c\rangle$ are both 2.5×10^{-9} s^{-1} (tracer is unitless), and the curl of these components is 6.5×10^{3} s^{-1} and 6.7×10^{3} s^{-1}, respectively.

The symmetric ("diffusive") part of the that tensor can be conveniently diagonalized by rotating the local coordinate through an angle θ (Kamenkovich *et al.*, 2015; Rypina *et al.*, 2012):

$$\boldsymbol{K}_s=\begin{pmatrix}\lambda_1 & 0\\ 0 & \lambda_2\end{pmatrix} \tag{6}$$

The angle θ defines the direction of the maximal tracer spreading, and the first eigenvalue is the spreading rate in this direction. The second eigenvalue corresponds to the spreading rate in the direction perpendicular to the maximal one. Both eigenvalues are real.

4.1 Polarity and time dependence

An intriguing new feature of the comprehensive **K**-tensor is the persistence of pairs of positive and negative eigenvalues λ_1 and λ_2 (Figs. 1-2), which we will refer to as "polarity". Many previous studies excluded negative diffusivities, either by using asymptotic estimates based on particle trajectories (Kamenkovich *et al.*, 2015; Rypina *et al.*, 2012) or by explicitly neglecting negative eigenvalues in the diffusivity tensor (Bachman *et al.*, 2020). Polar eigenvalues imply that the tracer concentration anomalies are being stretched in one direction and squeezed in the direction normal to that, leading to transient filamentation of the tracer field. Moreover, the polarity, which is ubiquitous in both QG and GCM solutions, is a robust feature of the instantaneous flow and is observed regardless of whether and how the rotational component of $\boldsymbol{F}$ is removed.

All components of the comprehensive tensor have significant time dependence, with the standard deviations comparable with and exceeding the corresponding time-mean values (Fig.3). The uncovered time dependence has important implications not only for transient tracer behavior, but also for time-mean tracer structure. The latter point can be illustrated by the time-average eddy flux $\overline{\boldsymbol{F}_{div}}$. To see this, we can write the time average of (1) in two different ways:

$$\overline{\boldsymbol{F}_{div}} = -\overline{\boldsymbol{K}}\boldsymbol{\nabla}\overline{\langle c\rangle} - \overline{\boldsymbol{K}'\boldsymbol{\nabla}\langle c'\rangle},\ \ \boldsymbol{K}' = \boldsymbol{K} - \overline{\boldsymbol{K}},\ \ c' = c - \bar{c} \quad \text{or} \quad \overline{\boldsymbol{F}_{div}} = -\widetilde{\boldsymbol{K}}\boldsymbol{\nabla}\overline{\langle c\rangle}. \qquad (4)$$

The above relation implies that (i) $\boldsymbol{K}'$ is at least as important as $\overline{\boldsymbol{K}}$; and (ii) $\widetilde{\boldsymbol{K}}$ is different from $\overline{\boldsymbol{K}}$. Both properties are confirmed by our calculations. The most practical approach for the parametrization is then unclear. If time-dependent ***K****(x,y,t)* is used, $\overline{\boldsymbol{F}_{div}}$ will depend on the accuracy of simulating tracer variance, whereas using $\widetilde{\boldsymbol{K}}$ can distort the important variability in $\boldsymbol{F}_{div}$.

Due to the non-stationary nature of the **K**-tensor, the sign of its eigenvalues and the corresponding angle θ both change in time. Although the polarity is reduced in $\overline{\boldsymbol{K}}$ and $\widetilde{\boldsymbol{K}}$, it continues to be observed even in these fields (not shown), which implies that eddies lead to persistent filamentation. As the sharpening of tracer gradients cannot continue forever, the effects of eddies have to be eventually balanced by the large-scale advection and small-scale diffusion. Persistent upgradient eddy potential vorticity fluxes (negative diffusivity) have indeed been reported in the eastward extensions of the Kuroshio (Waterman *et al.*, 2011; Waterman &

Jayne, 2011) and Gulf Stream (Shevchenko & Berloff, 2015); these studies, however, did not report the diffusivity tensor and the sign of the along-flow diffusivity. Another possibility is that negative eigenvalues are associated with non-divergent, rotational component of $\boldsymbol{K}_s\nabla\langle c\rangle$. Regardless of the origin and interpretation of the polarity, neglecting the negative values can potentially lead to serious biases in the eddy fluxes and tracer distributions.

4.3 Dependence on tracers

Another unexpected property of the comprehensive K-tensor is the dependence of its symmetric ("diffusive") component on the tracer field (Sun, 2020), which implies that $\boldsymbol{K}_s(x,y,t)$ is not uniquely determined by the flow and exists for each tracer pair separately; see also Bachman *et al.* (2020). As the manifestation of this property, the ensemble standard deviation for the first eigenvalue λ_1 of the symmetric tensor $\boldsymbol{K}_s$, calculated for among various pairs of tracers exceeds the ensemble mean in most of the domain (Figs. 4 and 5). Even more significantly, the spread in the values of the diffusive-flux divergence $\nabla \cdot \boldsymbol{K}_s\nabla\langle c\rangle$ is large (not shown).

The rotational component can be naturally suspected of being the cause of the above non-uniqueness of the K-tensor. Nevertheless, our results demonstrate that the non-uniqueness is not significantly reduced when the rotational component is removed for a general set of tracers: the non-uniqueness is similar in magnitude for $\boldsymbol{F}$ and $\boldsymbol{F}_{div}$ in both the QG and GCM simulations (Fig. 4c-f). On the other hand, any pair of initially linear (constant gradient) tracers must lead to the same diffusivity from $\boldsymbol{F}_{div}$ (see Methods), which can conveniently serve as a test of how well the rotational component is removed. Indeed, in this case the ensemble spread is reduced dramatically (Fig.4a-b).

5 Implications for eddy parameterization and diffusivity estimates

Using the exact solution for $\boldsymbol{K}(x,y,t)$ from (1) would lead to an accurate representation of the eddy-flux divergence for the given tracer pair, regardless of how and whether the rotational component is removed. An ultimate goal of the diffusion-based description of the eddy-induced transports is, however, parameterization of $\boldsymbol{K}(x,y,t)$ in terms of large-scale currents and stratification, that is, arrival at some generalized "turbulence closure". The corresponding approximate tensor $\boldsymbol{K}_p \approx \boldsymbol{K}(x,y,t)$ is intended to reproduce the most important effects of eddies on the large-scale tracer fields, without explicitly resolving the mesoscale. The uncovered complexity of the diffusivity tensor implies that the parameterized eddy flux divergence $-\nabla \cdot \boldsymbol{K_p} \nabla \langle c \rangle$ will inevitably contain biases with respect to $\boldsymbol{\nabla} \cdot \boldsymbol{F}$, but the significance of these biases for tracer distribution remains to be studied. These biases can be particularly hard to control, since the diffusive flux will have a large rotational component which affects the K-tensor estimates, according to our analysis. Since an exact match between $\boldsymbol{K_p}$ and $\boldsymbol{K}$ is practically impossible, it is important to estimate what properties of the diffusivity tensor are the most important for tracer distribution. This study describes several examples of such properties.

K-tensor depends on the flow decomposition (definition of the large-scale <…>), which is loosely defined in most cases. This study defines mesoscale based on spatial rather than temporal scales, which is more directly relevant to the issue of its parameterization in numerical models. The spatial filter characteristics cannot, however, be easily derived from model resolution alone, since it is unclear to what extent different dynamical scales are actually resolved. K-tensor is also non-stationary, and a meaningful definition of $\boldsymbol{K_p}$ will depend on the time scales of large-scale tracer variability. The analysis of the dominant spatial and temporal scales will need to be carried out in each particular case. Negative eigenvalues in the tensor and the potential importance of all tensor components dramatically complicates the definition of the closure. These negative diffusivities are, however, transient, and the corresponding direction of spreading constantly changes in time. The importance of this variability needs to be assessed. In addition, the effects of negative eigenvalues can be fully compensated by the skew part of the diffusivity tensor, which is divergent and, thus, also plays a role in tracer distribution. Observation-based estimates, on the other hand, present additional challenges. Given the discovered complexity, obtaining accurate estimates of $\boldsymbol{K}$ from drifter and float trajectories (Lagrangian observations) appears highly problematic, because these asymptotic and spatially nonlocal methods will not be able to accurately capture the spatial and temporal variability of the **K**-tensor.

Finally, the comprehensive diffusivity tensor is a function of the tracer field, formally violating assumptions of the classical, tracer-independent flux-gradient relation. A practical approach to this problem is to use multi-tracer ensemble-averaged estimates of **K** (Bachman *et al.*, 2020; Bachman *et al.*, 2017), but the corresponding and unavoidable biases for each given tracer pair remain to be assessed and understood. An alternative solution is to expand the traditional flux-gradient representation of the eddy flux by adding new, non-diffusive terms. Such expansion can involve terms that explicitly depend on either the tracer concentration or its curvature, as well as purely stochastic components. Note that the latter stochastic component can be expected to be effectively removed by using the multi-tracer method.

Since the most important properties and aspects of $\boldsymbol{K_p}$ remain to be identified, we do not yet know to what extent they are affected by the full tensor properties described in this study. Although it is tempting to conclude that the only the direct resolution of the mesoscale can lead to accurate tracer simulations, we must realize that the task of its parameterization will remain relevant for some time.

Acknowledgments and Data

Kamenkovich and Lu were supported by NOAA grant NA16OAR4310165 and NSF grant 1849990. The authors declare no conflicts or competing interests. Berloff gratefully acknowledges funding by NERC, UK Grants $NE/R011567/1$ and $NE/T002220/1$, and by Leverhulme Trust, UK Grant $RPG-2019-024$, and by the Moscow Center for Fundamental and Applied Mathematics (supported by the Agreement 075-15−2019−1624 with the Ministry of Education and Science of the Russian Federation). I.K. would like to thank Zulema Garraffo for the continuous help with the offline HYCOM model; P.B., M.H. and L.S. would like to thank James McWilliams for fruitful discussions on the topics of this study. Model data used to produce figures in this study are available from (URL site will be included here); additional data are available from the corresponding author upon request.

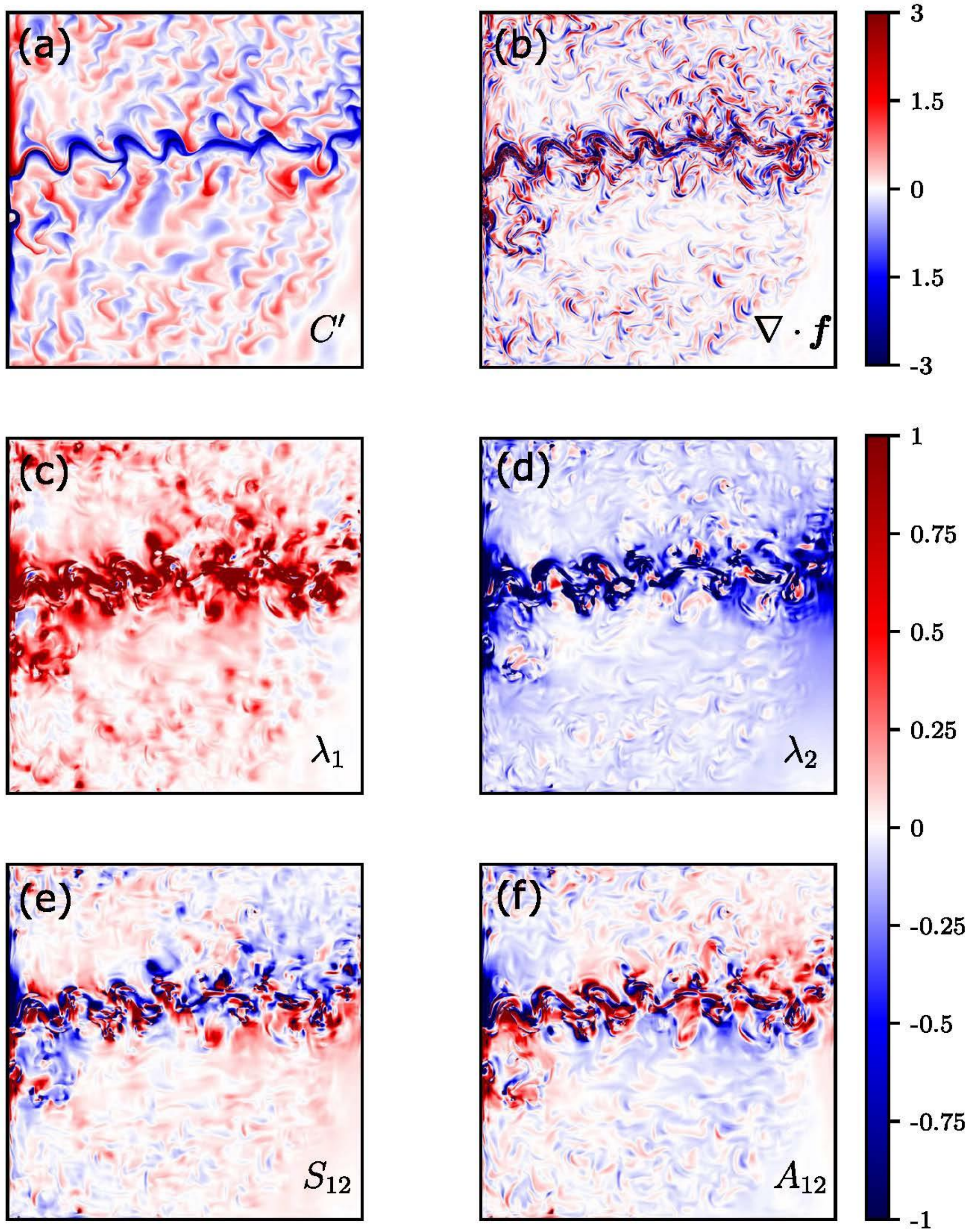

Figure 1: Results of the QG simulations at day 183: (a) tracer anomaly c'=c(x,y,t)-c(x,y,0); (b) divergence of the tracer flux (tracer units times 10^{-6} s^{-1}); (c)-(d) eigenvalues and (e)-(f) off-diagonal terms of the diffusivity tensor (units are 10^4 m^2s^{-1}).

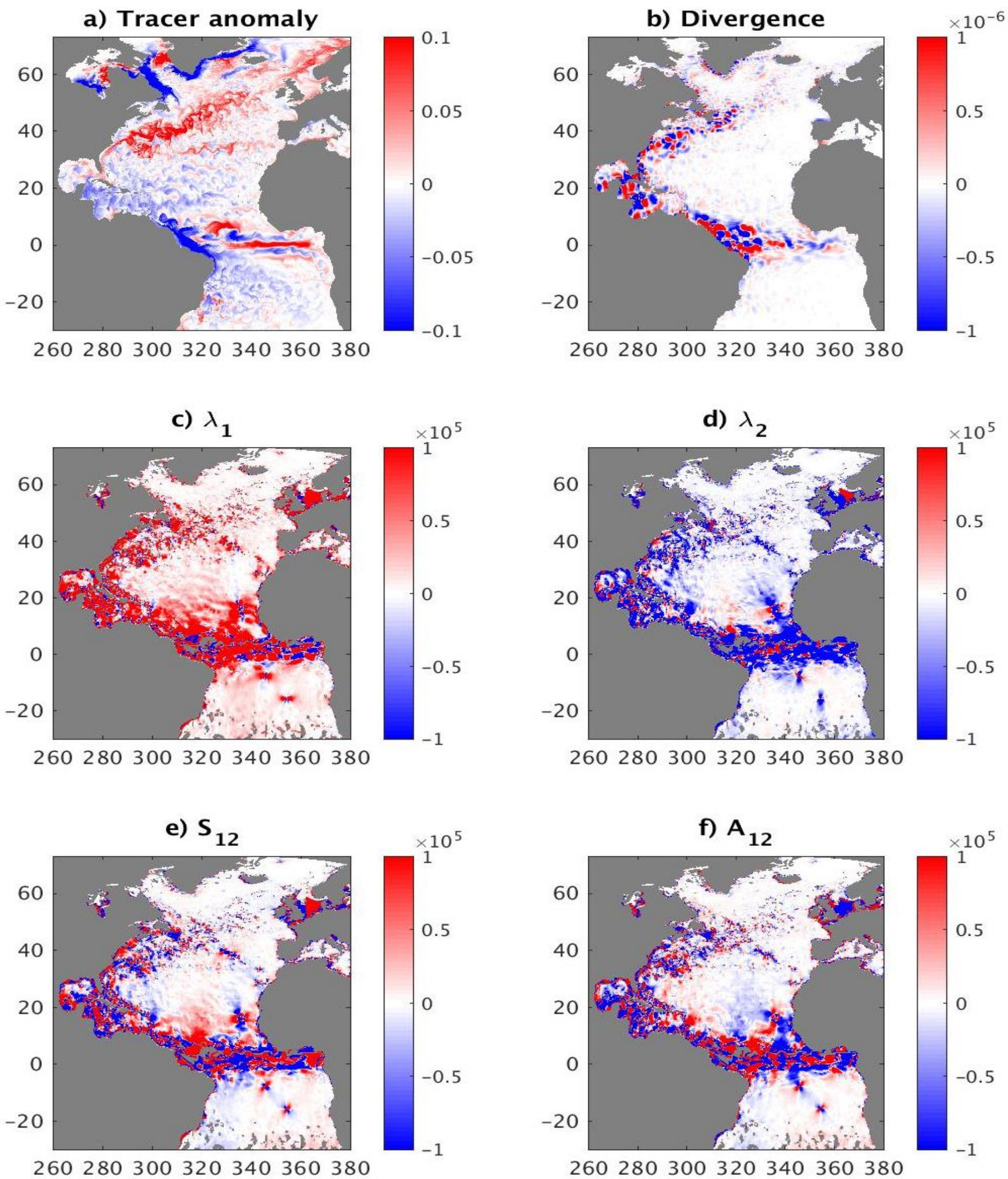

Figure 2: Results of the GCM simulations, layer 17 (depth of approximately 300-600 m): (a) tracer anomaly c'=*c(x,y,t)-c(x,y,0)* (tracer is unitless); (b) divergence of the tracer flux (units are s^{-1}) averaged over days 341-350 of year 1; (c)-(d) eigenvalues and (e)-(f) off-diagonal terms of the diffusivity tensor (units are m^2s^{-1}), derived from the eddy fluxes and tracer gradients averaged over days 341-350 of year 1. Note large values in the tropics due to weak tracer gradients and, possibly, long Rossby deformation radius. Regions near the open boundaries, where the tracer concentrations are initially set to zero are masked.

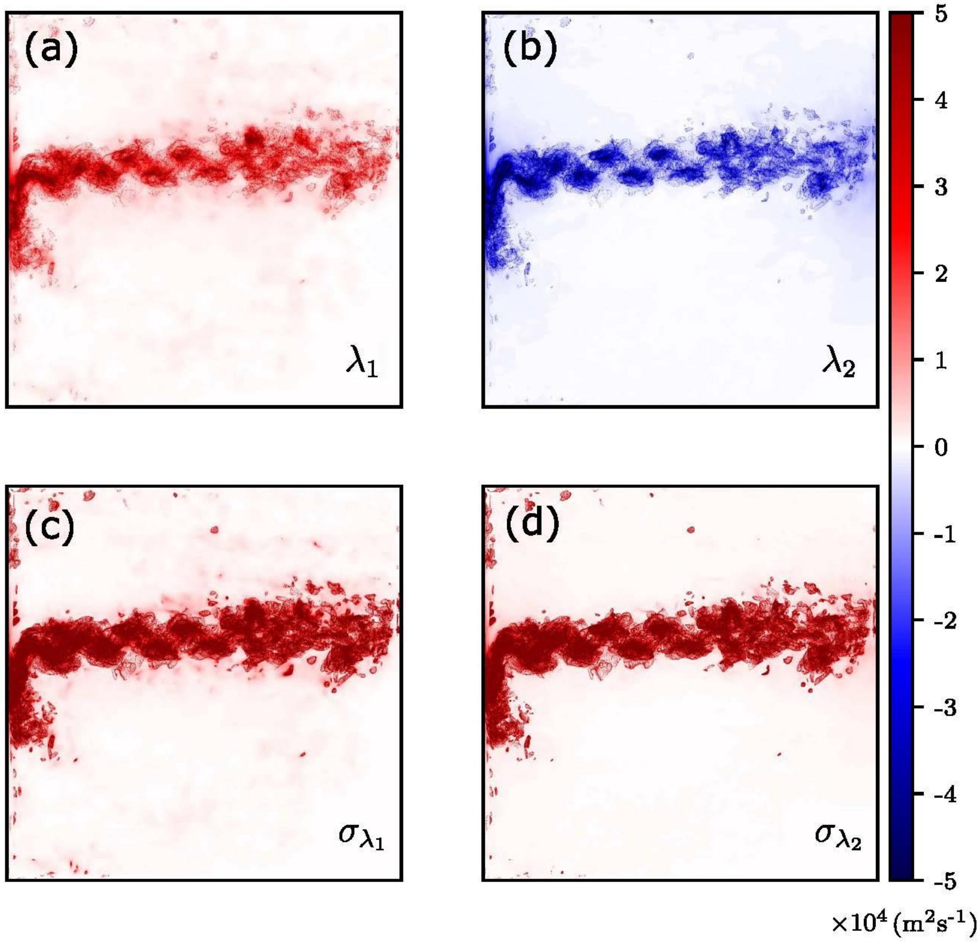

Figure 3: Time-dependence in the eigenvalues $\lambda_1$and λ_2 of the diffusivity tensor in the QG simulations over the period of 183 days. Panels (a-b) show the time-mean values, panels (c-d) – standard deviations. Time-means of eigenvalues over 183 days.

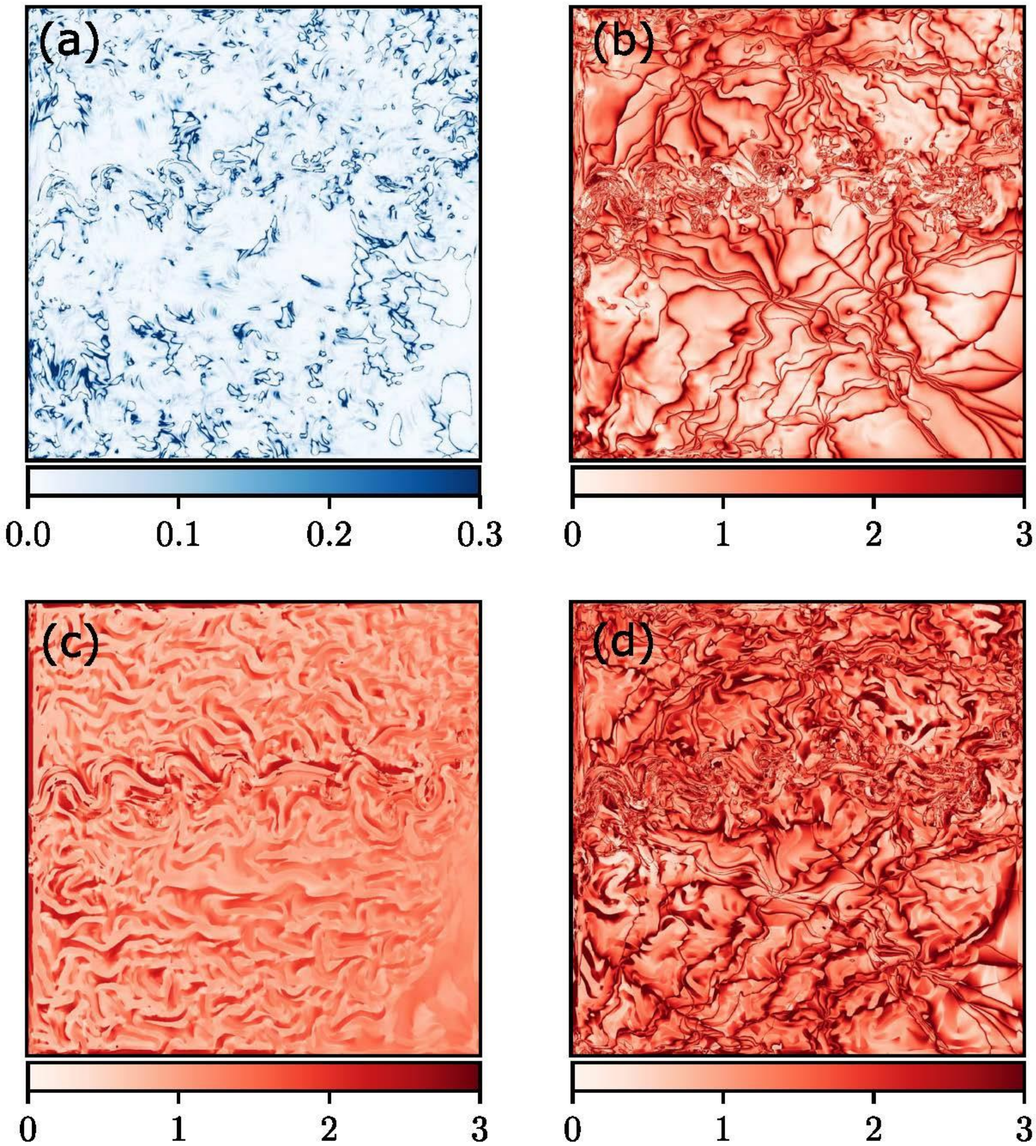

Figure 4: Non-uniqueness of the K-tensor (tracer dependence) in the QG simulations (day 183), for the ensemble of 15 tracer pairs. It is shown as the ensemble standard deviation divided by the ensemble mean for the first eigenvalue λ_1, calculated for $\mathbf{F_{div}}$ (left column) and $\mathbf{F}$ (right column): (a-b) Linear tracers in the QG model; (c-d) Nonlinear tracers in the QG model.

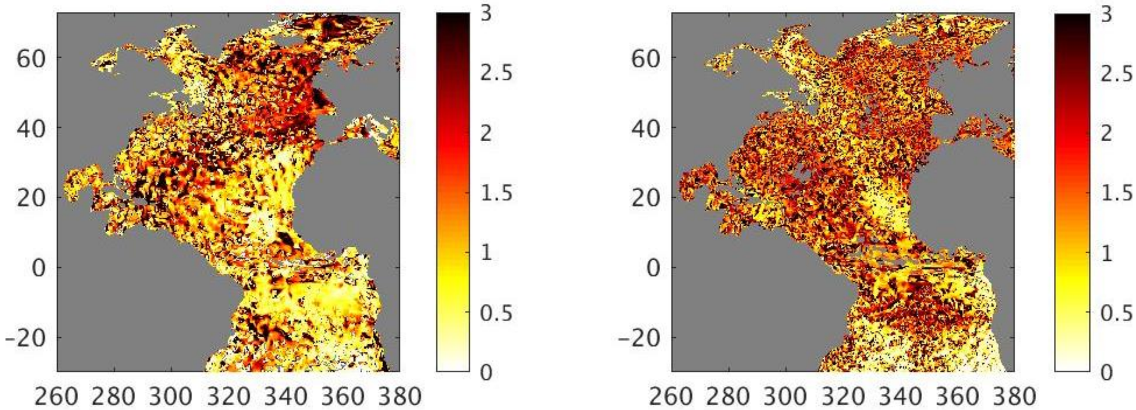

Figure 5: Non-uniqueness (tracer dependence) of the **K**-tensor in the HYCOM simulations, for the ensemble of 6 tracer pairs. It is shown as the ensemble standard deviation divided by the ensemble mean for the first eigenvalue λ_1, calculated for $\mathbf{F_{div}}$ (left column) and **F** (right column). The tensor is derived from the eddy fluxes and tracer gradients averaged over days 341-350 of year 1

References

Abernathey, R. P., & Marshall, J. (2013), Global surface eddy diffusivities derived from satellite altimetry, *J Geophys Res-Oceans*, *118*(2), 901-916, doi:10.1002/jgrc.20066.

Bachman, S. D., Fox-Kemper, B., & Bryan, F. O. (2015), A tracer-based inversion method for diagnosing eddy-induced diffusivity and advection, *Ocean Model*, *86*, 1-14, doi:10.1016/j.ocemod.2014.11.006.

Bachman, S. D., Fox-Kemper, B., & Bryan, F. O. (2020), A Diagnosis of Anisotropic Eddy Diffusion From a High-Resolution Global Ocean Model, *J Adv Model Earth Sy*, *12*(2), doi:10.1029/2019MS001904.

Bachman, S. D., Marshall, D. P., Maddison, J. R., & Mak, J. (2017), Evaluation of a scalar eddy transport coefficient based on geometric constraints, *Ocean Model*, *109*, 44-54, doi:10.1016/j.ocemod.2016.12.004.

Bleck, R. (2002), An Oceanic general circulation model framed in hybrid isopycnic-Cartesian coordinates (vol 4, pg 55, 2002), *Ocean Model*, *4*(2), 219-219, doi:Pii S1463-5003(01)00017-8
Doi 10.1016/S1463-5003(01)00017-8.

Busecke, J. J. M., & Abernathey, R. P. (2019), Ocean mesoscale mixing linked to climate variability, *Sci Adv*, *5*(1), doi:ARTN eaav5014
10.1126/sciadv.aav5014.

Canuto, V. M., Cheng, Y., Howard, A. M., & Dubovikov, M. S. (2019), Three-Dimensional, Space-Dependent Mesoscale Diffusivity: Derivation and Implications, *J Phys Oceanogr*, *49*(4), 1055-1074, doi:10.1175/Jpo-D-18-0123.1.

Chassignet, E. P., Smith, L. T., Halliwell, G. R., & Bleck, R. (2003), North Atlantic Simulations with the Hybrid Coordinate Ocean Model (HYCOM): Impact of the vertical coordinate choice, reference pressure, and thermobaricity, *J Phys Oceanogr*, *33*(12), 2504-2526, doi:Doi 10.1175/1520-0485(2003)033<2504:Naswth>2.0.Co;2.

Chelton, D. B., Schlax, M. G., Samelson, R. M., & de Szoeke, R. A. (2007), Global observations of large oceanic eddies, *Geophys Res Lett*, *34*(15), doi:Artn L15606

10.1029/2007gl030812.

Cole, S. T., Wortham, C., Kunze, E., & Owens, W. B. (2015), Eddy stirring and horizontal diffusivity from Argo float observations: Geographic and depth variability, *Geophys Res Lett*, *42*(10), 3989-3997, doi:10.1002/2015gl063827.

Delworth, T. L., Rosati, A., Anderson, W., Adcroft, A. J., Balaji, V., Benson, R., et al. (2012), Simulated Climate and Climate Change in the GFDL CM2.5 High-Resolution Coupled Climate Model, *J Climate*, *25*(8), 2755-2781, doi:10.1175/Jcli-D-11-00316.1.

Eden, C. (2007), Eddy length scales in the North Atlantic Ocean, *J Geophys Res-Oceans*, *112*(C6), doi:Artn C06004 10.1029/2006jc003901.

Eden, C., & Greatbatch, R. J. (2009), A diagnosis of isopycnal mixing by mesoscale eddies, *Ocean Model*, *27*(1-2), 98-106, doi:10.1016/j.ocemod.2008.12.002.

Gnanadesikan, A., Bianchi, D., & Pradal, M. A. (2013), Critical role for mesoscale eddy diffusion in supplying oxygen to hypoxic ocean waters, *Geophys Res Lett*, *40*(19), 5194-5198, doi:10.1002/grl.50998.

Griesel, A., Gille, S. T., Sprintall, J., McClean, J. L., LaCasce, J. H., & Maltrud, M. E. (2010), Isopycnal diffusivities in the Antarctic Circumpolar Current inferred from Lagrangian floats in an eddying model, *J Geophys Res-Oceans*, *115*, doi:10.1029/2009jc005821.

Haigh, M., Sun, L., Shevchenko, I., & Berloff, P. (2020), Tracer-based estimates of eddy-induced diffusivities, *Deep-Sea Res Pt I*, *160*, doi:10.1016/j.dsr.2020.103264.

Jayne, S. R., & Marotzke, J. (2002), The oceanic eddy heat transport, *J Phys Oceanogr*, *32*(12), 3328-3345, doi:Doi 10.1175/1520-0485(2002)032<3328:Toeht>2.0.Co;2.

Kamenkovich, I., Berloff, P., & Pedlosky, J. (2009), Anisotropic Material Transport by Eddies and Eddy-Driven Currents in a Model of the North Atlantic, *J Phys Oceanogr*, *39*(12), 3162-3175, doi:10.1175/2009jpo4239.1.

Kamenkovich, I., Garraffo, Z., Pennel, R., & Fine, R. A. (2017), Importance of mesoscale eddies and mean circulation in ventilation of the Southern Ocean, *J Geophys Res-Oceans*, *122*(4), 2724-2741, doi:10.1002/2016jc012292.

Kamenkovich, I., Rypina, I. I., & Berloff, P. (2015), Properties and Origins of the Anisotropic Eddy-Induced Transport in the North Atlantic, *J Phys Oceanogr*, *45*(3), 778-791, doi:10.1175/Jpo-D-14-0164.1.

Karabasov, S. A., Berloff, P. S., & Goloviznin, V. M. (2009), CABARET in the ocean gyres, *Ocean Model*, *30*(2-3), 155-168, doi:10.1016/j.ocemod.2009.06.009.

Lau, N. C., & Wallace, J. M. (1979), Distribution of Horizontal Transports by Transient Eddies in the Northern Hemisphere Wintertime Circulation, *J Atmos Sci*, *36*(10), 1844-1861, doi:Doi 10.1175/1520-0469(1979)036<1844:Otdoht>2.0.Co;2.

Li, Z. J., Chao, Y., & McWilliams, J. C. (2006), Computation of the streamfunction and velocity potential for limited and irregular domains, *Mon Weather Rev*, *134*(11), 3384-3394, doi:Doi 10.1175/Mwr3249.1.

Lumpkin, R., Treguier, A. M., & Speer, K. (2002), Lagrangian eddy scales in the Northern Atlantic Ocean, *J Phys Oceanogr*, *32*(9), 2425-2440, doi:Doi 10.1175/1520-0485-32.9.2425.

Maddison, J. R., Marshall, D. P., & Shipton, J. (2015), On the dynamical influence of ocean eddy potential vorticity fluxes, *Ocean Model*, *92*, 169-182, doi:10.1016/j.ocemod.2015.06.003.

Marshall, J., Shuckburgh, E., Jones, H., & Hill, C. (2006), Estimates and implications of surface eddy diffusivity in the Southern Ocean derived from tracer transport, *J Phys Oceanogr*, *36*(9), 1806-1821, doi:Doi 10.1175/Jpo2949.1.

Marshall, J., & Shutts, G. (1981), A Note on Rotational and Divergent Eddy Fluxes, *J Phys Oceanogr*, *11*(12), 1677-1680, doi:Doi 10.1175/1520-0485(1981)011<1677:Anorad>2.0.Co;2.

McClean, J. L., Poulain, P. M., Pelton, J. W., & Maltrud, M. E. (2002), Eulerian and lagrangian statistics from surface drifters and a high-resolution POP simulation in the North Atlantic, *J Phys Oceanogr*, *32*(9), 2472-2491, doi:Doi 10.1175/1520-0485-32.9.2472.

McWilliams, J. (2008), The nature and consequences of oceanic eddies, in *Eddy-Resolving Ocean Modeling*, edited by M. Hecht and H. Hasumi, pp. 131-147, AGU Monographs.

O'Dwyer, J., Williams, R. G., LaCasce, J. H., & Speer, K. G. (2000), Does the potential vorticity distribution constrain the spreading of floats in the North Atlantic?, *J Phys Oceanogr*, *30*(4), 721-732, doi:Doi 10.1175/1520-0485(2000)030<0721:Dtpvdc>2.0.Co;2.

Prandtl (1925), Bericht über untersuchungen zur ausgebildeten turbulenz, *Z. Angew. Math. Mech.*, *5*, 136-139.

Roberts, M. J., & Marshall, D. P. (2000), On the validity of downgradient eddy closures in ocean models, *J Geophys Res-Oceans*, *105*(C12), 28613-28627, doi:Doi 10.1029/1999jc000041.

Rypina, I. I., Kamenkovich, I., Berloff, P., & Pratt, L. J. (2012), Eddy-Induced Particle Dispersion in the Near-Surface North Atlantic, *J Phys Oceanogr*, *42*(12), 2206-2228, doi:10.1175/Jpo-D-11-0191.1.

Sallee, J. B., Speer, K., Morrow, R., & Lumpkin, R. (2008), An estimate of Lagrangian eddy statistics and diffusion in the mixed layer of the Southern Ocean, *J Mar Res*, *66*(4), 441-463, doi:Doi 10.1357/002224008787157458.

Shevchenko, I. V., & Berloff, P. S. (2015), Multi-layer quasi-geostrophic ocean dynamics in Eddy-resolving regimes, *Ocean Model*, *94*, 1-14, doi:10.1016/j.ocemod.2015.07.018.

Sun, L., M. Haigh, P. Berloff, and I, Kamenkovich (2020), On non-uniqueness of the mesoscale eddy diffusivity, *J. Fluid Mech.*, *under review*.

Taylor (1921), Diffusion by continuous movements, *Proc. London Math. Soc.*, *20*, 196-211.

Vallis, G. (2017), *Atmospheric and oceanic fluid dynamics*.

Waterman, S., Hogg, N. G., & Jayne, S. R. (2011), Eddy-Mean Flow Interaction in the Kuroshio Extension Region, *J Phys Oceanogr*, *41*(6), 1182-1208, doi:10.1175/2010jpo4564.1.

Waterman, S., & Jayne, S. R. (2011), Eddy-Mean Flow interactions in the Along-Stream Development of a Western Boundary Current Jet: An Idealized Model Study, *J Phys Oceanogr*, *41*(4), 682-707, doi:10.1175/2010jpo4477.1.

Wiebe, E. C., & Weaver, A. J. (1999), On the sensitivity of global warming experiments to the parametrisation of sub-grid scale ocean mixing, *Clim Dynam*, *15*(12), 875-893, doi:DOI 10.1007/s003820050319.

Williams, K. D., Harris, C. M., Bodas-Salcedo, A., Camp, J., Comer, R. E., Copsey, D., et al. (2015), The Met Office Global Coupled model 2.0 (GC2) configuration, *Geosci Model Dev*, *8*(5), 1509-1524, doi:10.5194/gmd-8-1509-2015.